Electronic and Charge-Transport Properties of the Au3(CH3NCOCH3)3 Crystal: A Density Functional Theory Study

ARTICLE *in* JOURNAL OF PHYSICAL CHEMISTRY LETTERS · JULY 2013

Impact Factor: 7.46 · DOI: 10.1021/jz400950v

THE JOURNAL OF PHYSICAL CHEMISTRY Letters

Letter

pubs.acs.org/JPCL

Electronic and Charge-Transport Properties of the $Au_3(CH_3N{=}COCH_3)_3$ Crystal: A Density Functional Theory Study

Lingyun Zhu,[†,§] Veaceslav Coropceanu,[†] Yuanping Yi,[†,∥] Bhaskar Chilukuri,[‡] Thomas R. Cundari,[‡] and Jean-Luc Brédas*[,†,⊥]

[†]School of Chemistry and Biochemistry and Center for Organic Photonics and Electronics, Georgia Institute of Technology, Atlanta, Georgia 30332-0400, United States

[‡]Department of Chemistry Center for Advanced Scientific Computing and Modeling (CASCaM), University of North Texas, Denton, Texas 76203, United States

Supporting Information

ABSTRACT: Density functional theory was used to investigate the electronic and charge-transport properties of the trinuclear gold $Au_3(CH_3N{=}COCH_3)_3$ crystal. Hole transport is found to be anisotropic and characterized by a very small effective mass of about 0.21 m_0 along the stacking direction of the Au_3 molecules. Interestingly, the calculations suggest an isotropic character of electron transport, for which the effective mass is about 1 m_0. We show that while the interstack interactions facilitate electron transport in the directions perpendicular to the stacks, they act to diminish this transport along the stacking directions. Overall, the present results indicate that this compound is a promising ambipolar material for application in electronic devices.

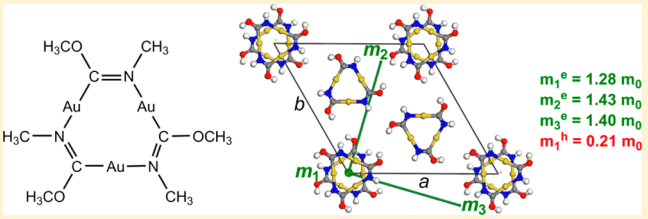

SECTION: Energy Conversion and Storage; Energy and Charge Transport

Gold-trimer based systems have recently received significant attention due to their interesting properties[1−3] related to π-acidity and basicity, luminescence, thermochromism, or solvoluminescence, and their potential for applications in metal−organic electronic devices.[4,5] For instance, upon irradiation with UV light, tris((μ2-methylimino(methoxy)-methyl)-gold(I)) ($Au_3(CH_3N{=}COCH_3)_3$) exhibits a long-lived yellow emission with a lifetime of about 31 s; in addition, when a previously photoirradiated crystal $Au_3(CH_3N{=}COCH_3)_3$ is dropped into a good solvent, a bright burst of yellow light detectable by the human eye is produced (solvoluminescence).[6−8] In general, $Au_3(CH_3N{=}COCH_3)_3$ can crystallize into three polymorphic forms: hexagonal, triclinic, and monoclinic.[7] The hexagonal polymorph is the only one that displays solvoluminescence and in which the gold(I) ions of $Au_3(CH_3N{=}COCH_3)_3$ form extended chains. It was suggested that solvoluminescence involves energy storage that is facilitated by charge-carrier mobility along the gold chains.[8] Despite significant interest in this system, only limited theoretical studies have been reported to date.[9,10]

Here, we use quantum mechanical methods to study the electronic and charge-transfer properties of the hexagonal form of the $Au_3(CH_3N{=}COCH_3)_3$ crystal. To the best of our knowledge, our work represents the first study of the charge-transport parameters in this class of materials.

The electronic-structure calculations on the crystal were performed at the density functional theory (DFT) level using the Perdew−Burke−Ernzerhof (PBE) exchange-correlation functional with a plane-wave basis set (300 eV cutoff) and projector augmented wave (PAW) potentials.[11,12] The self-consistent calculations were carried out with 4 × 4 × 14 and 4 × 4 × 8 k-point meshes for structures based on the original unit cell and a doubled unit cell, respectively. The inverse effective mass tensor for the three-dimensional crystal, m_{ji}^{-1}, is defined as

$$\frac{1}{m_{ij}} = \frac{1}{\hbar^2}\frac{\partial^2 E}{\partial k_j \partial k_i} \quad (1)$$

where subscripts i and j denote the Cartesian coordinates in reciprocal space, E is the band energy, $\hbar$ is the Planck constant, and k is the electron wavevector. The inverse effective mass tensor was calculated assuming dk = 0.01/Bohr. All the DFT crystal-structure calculations were carried out using the VASP 5.2 code.[13]

The transfer integrals (electronic couplings) were evaluated by using a fragment orbital approach in combination with a basis set orthogonalization procedure.[14] Since the frontier valence levels of $Au_3(CH_3N{=}COCH_3)_3$ are 2-fold degenerate (labeled here as H and H-1), the electronic couplings for holes are evaluated by considering effective transfer integrals defined as

$$t_h^{\text{eff}} = [(t_{H,H}{}^2 + t_{H\text{-}1,H}{}^2 + t_{H,H\text{-}1}{}^2 + t_{H\text{-}1,H\text{-}1}{}^2)/2]^{1/2} \quad (2)$$

Received: May 6, 2013
Accepted: June 18, 2013
Published: June 18, 2013

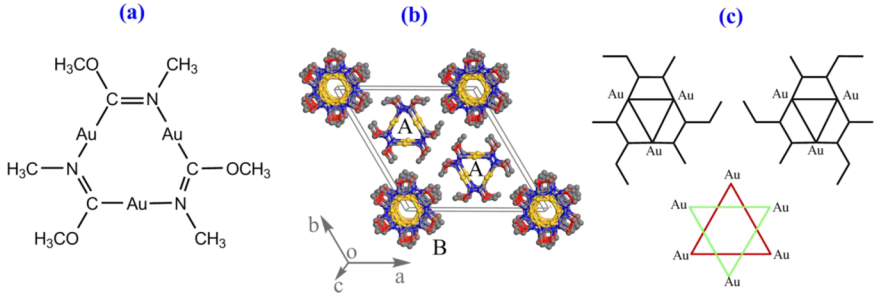

Figure 1. (a) Chemical structure of the investigated system; (b) original crystal structure; (c) top: illustration of the flip disorder that leads to two alternate positions for the methoxy-methyl groups; bottom: illustration of the two possible positions of the Au_3 triangles in the B stacks.

The transfer-integral calculations were performed at the B3LYP level with the LAN2DZ basis set for the gold atoms and the 6-31G(d,p) basis set for the other atoms. All DFT molecular calculations were carried out using the Gaussian 09 package.[15] Since the methoxy and methyl groups do not play any significant role in the frontier molecular orbitals, they have been replaced in all calculations with OH and H, respectively.

The $Au_3(CH_3N{=}COCH_3)_3$ hexagonal polymorph structure[6] belongs to the *P6/m* space group with cell parameters a = 19.41 Å, b = 19.41 Å, c = 3.3463 Å, α = 90°, β = 90°, and γ = 120° (see Figure 1). The molecules stack cofacially along the c-direction. Two types of stacks, referred to as A and B, are present in the unit cell.[8] Stacks A are prismatic with ordered gold triangles and intermolecular gold distances of 3.346 Å. For each pair of A stacks, there exists a B stack in which there are two sets of gold triangles positioned with an offset of 60 degrees. However, the crystal structure data suggest that the gold triangles in stacks B are not ordered but rather exhibit a significant positional disorder between these two rotational configurations. There can be additional disorder in both types of stacks due to two possible positions for the methoxy-methyl groups resulting from a flip of the molecules around a C_2 axis in the middle of the Au_3 triangle. In the absence of well-defined experimental crystal structures, seven structural models were generated (see Figure 2). In models 1 and 2, the gold triangles in stacks B alternate between the two rotational configurations: in model 1, the orientation of the methoxy-methyl groups is the same for all molecules, while in model 2 adjacent molecules in stacks A have different orientations of these groups. In order to delineate the difference between the effects that stacks A and B have on the charge-transport properties, models 3−5 were also considered, where either stacks A or stacks B have been excluded from the calculations. Finally, we also considered two models (models 6−7; see Figure S1 in the Supporting Information (SI)) where all stacks are prismatic (i.e., type A).

The calculated electronic band structures for models 1 and 2 are given in Figure 3 (see Figure S2 in the SI for all other results). In both cases, a very large dispersion is found along the stacking direction (Γ−A, H−K, and M−L) for both the valence band (VB) and conduction band (CB). In addition, a non-negligible band dispersion is also found for electrons in the *ab*-plane (K−Γ and Γ−M). As a consequence of the large band dispersions, the effective mass for holes is remarkably small (0.2 m_0; m_0 represents the free electron rest mass) along the stacking direction in both model structures. In contrast, the effective mass in the *ab*-plane is very large (4 to 39 m_0, see Table S1 in the SI). As a consequence, hole transport in the $Au_3(CH_3N{=}COCH_3)_3$ crystal is favorable only along the stacking direction. Interestingly, in the case of electrons, the

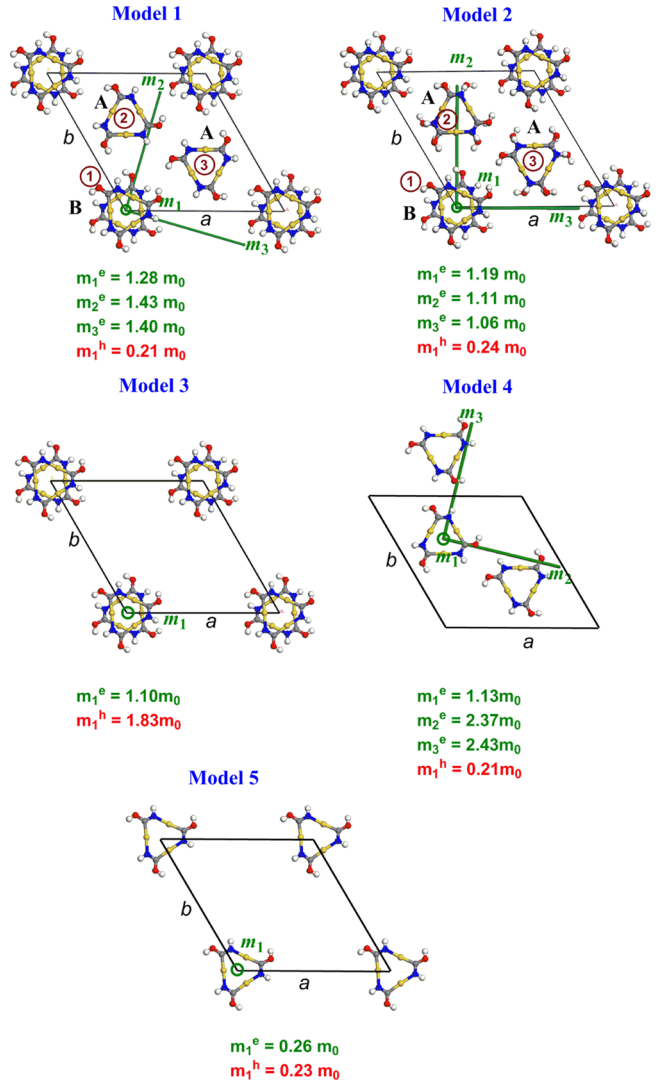

Figure 2. Illustration of the structural models used for the band-structure calculations (see SI for models 6 and 7). The green lines (in the *ab*-plane) and circle (⊥*ab* plane) indicate the directions of the principal components of m_{ji}^{-1} with the smallest effective-mass values. The effective masses for electrons (in green) and holes (in red) are given for each model; m_0 represents the free electron rest mass.

effective mass is nearly isotropic and characterized by relatively small values in the range of 1.1m_0 −1.4 m_0 (see Figure 2). Thus, in contrast to hole transport, electron transport is expected to display a three-dimensional character. The calculations based on the structural models where all stacks are prismatic (models

dx.doi.org/10.1021/jz400950v | J. Phys. Chem. Lett. 2013, 4, 2186−2189

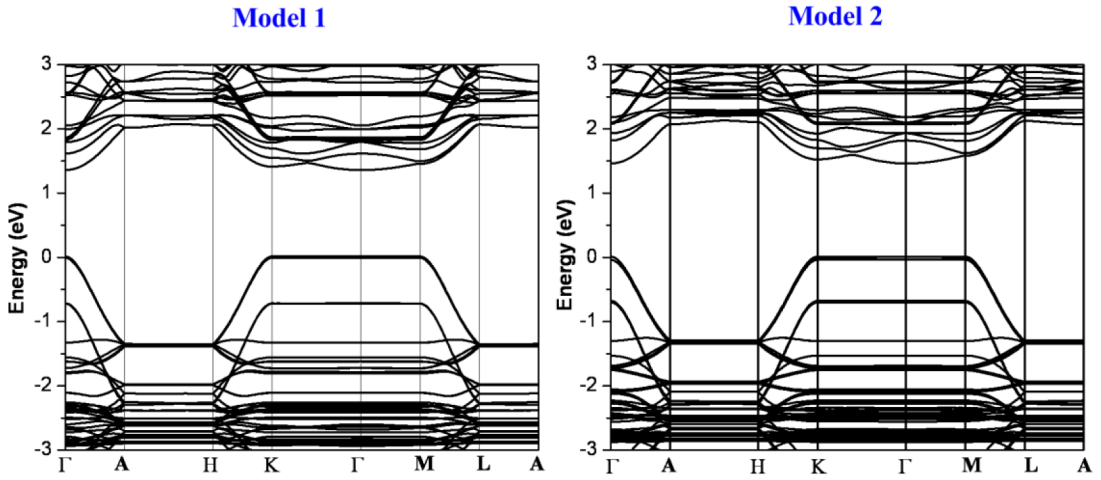

Figure 3. Calculated electronic band structure of Models 1 and 2. The points of high symmetry in the first Brillouin zone are labeled as follows: Γ = (0, 0, 0), *A* = (0, 0, 1/2), *H* = (1/3, 2/3, 1/2), *K* = (1/3, 2/3, 0), *M* = (0, 1/2, 0), and *L* = (0, 1/2, 1/2), all in crystallographic coordinates. The zero of energy is given at the top of the valence band.

6−7; see SI) lead to similar conclusions. This indicates that the existence of two set of Au_3 cluster morphologies in stacks B play a marginal effect on the overall transport properties of both holes and electrons. The comparison of the results derived for structures 1 and 2 indicate that the disorder related to the positions of the methoxy-methyl groups also plays only a small effect on the hole and electron transport properties.

In order to better separate the effects of stacks A and B on the electronic and transport properties, models 3 and 4 were also considered. The band structure results are given in the SI while the corresponding effective masses are shown in Figure 2. The results reveal that in the case of holes, the effective mass along stacks B is about 9 times larger than that along stacks A. This result can be explained by the fact that, in the cofacial dimers that are characteristic of stacks A, the overlap of the wave functions, and consequently the electronic coupling, should be larger than in stack-B dimers where there is rotational mismatch of the adjacent gold triangles.

The results for electron transport are less straightforward to rationalize. On one hand, the removal of B stacks leads to an increase of the effective mass in the *ab*-plane by about a factor of 2, which can be related to the presence of fewer coupling channels. On the other hand, the effective mass along the B stacks is in fact slightly smaller than that along the A stacks, which is in contradiction with the argument made above for holes. These findings suggest that, in the case of electron transport, there occurs a competition between interstack and intrastack interactions. This conclusion is supported by the results obtained for model 5 in which all dimers are cofacial and the interstack interactions are lacking; in this case, the effective mass for electrons is actually very small and similar to that derived for holes.

In order to understand how the interstack interactions affect the electron effective mass along the stacking direction, we evaluated the electronic couplings for different transport pathways. The results are collected in Table 1. These calculations indicate that the electronic couplings along stacks A are very large for both holes and electrons, about 440 and 480 meV, respectively. The electronic couplings along stacks B are about 100 meV for holes and 210 meV for electrons. We note that the electronic couplings for electrons are larger than for holes along both stacks. In the case of holes, in agreement

Table 1. B3LYP Transfer Integrals (t) Calculated for the $Au_3(CH_3N{=}COCH_3)_3$ Crystal[a]

model	pair	t_0(holes)/meV	t_0(electrons)/meV
1	11′ (along c)	97	206
	22′= 33′ (along c)	441	478
	12=1′3′ (in *ab*-plane)	1	25
	13=1′2′ (in *ab*-plane)	4	88
	23=2′3′ (in *ab*-plane)	5	22
	12′	1	14
	13′	1	38
	23′	1	12
2	11′ (along *c*)	97	206
	22′= 33′ (along *c*)	382	455
	12 (in *ab*-plane)	1	25
	13 (in *ab*-plane)	4	88
	23 (in *ab*-plane)	5	22
	1′2′ (in *ab*-plane)	5	70
	1′3′ (in *ab*-plane)	1	44
	2′3′ (in *ab*-plane)	5	21

[a]The labeling of the molecular pairs as used is shown in Figure 2. The molecules in the *ab* plane are labeled as 1, 2, 3, etc., and the molecules in the lower layer along the stacking direction are labeled as 1′, 2′, 3′, etc.

with the band-structure results, only very small values are obtained for the interstack electronic couplings. As expected, significant interstack couplings are found for the electrons. Interestingly, the interstack couplings are significant not only between molecules located in the same *ab* plane but also between molecules belonging to different stacks and located in adjacent *ab*-planes. This result underlines that the increase in the effective mass for electrons, from its minimum value of 0.2 m_0 obtained with model 5 to 1.2−1.3 m_0 for a more realistic crystal structure given by models 1 and 2, is due to a destructive interference among the intrastack and interstack electronic coupling pathways. By contrast, the effective mass for holes is entirely defined by the intrastack couplings.

Finally, in order to shed some light on the effect of structural disorder on the charge-transport properties, we investigated the effect of thermal disorder by considering the dependence of the transfer integrals on molecular rotations and molecular displacements. The results indicate that the holes are more

dx.doi.org/10.1021/jz400950v | *J. Phys. Chem. Lett.* 2013, 4, 2186−2189

strongly affected by structural fluctuations (see Figures S3 and S4). However, gaining a deeper understanding of the impact of dynamical disorder on the charge-transport properties would require a more detailed investigation of the electron (hole)−phonon coupling interactions, which is beyond the scope of the present work.

To summarize, our investigations of the electronic and charge-transport properties of the $Au_3(CH_3N{=}COCH_3)_3$ crystal show that this compound is characterized by a very small hole effective mass (0.21 m_0) along the stacking directions of the gold triangles. In the case of electrons, while the effective mass is about 5−6 times larger than in the case of holes, it remains relatively small (similar to that for holes and electrons in pentacene,[16] which is among the organic molecular semiconductors presenting the highest charge-carrier mobilities) and should allow efficient electron transport. In contrast to the holes that are confined to one-dimensional transport pathways, the electron transport is isotropic (three-dimensional). We suggest that this important difference in the pattern of delocalization might lead to the peculiar exciton features responsible for the observed solvoluminescence in $Au_3(CH_3N{=}COCH_3)_3$. Overall, our results indicate that this compound is a promising ambipolar material for application in electronic devices. Therefore, the investigation of the electron−phonon coupling mechanisms and the development of appropriate charge transport models for this class of systems will be of interest.

■ ASSOCIATED CONTENT

Supporting Information

Calculated band structures and the derived values of the effective masses of the investigated model structures. This material is available free of charge via the Internet at http://pubs.acs.org.

■ AUTHOR INFORMATION

Corresponding Author

*E-mail: jean-luc.bredas@chemistry.gatech.edu.

Present Addresses

[§]National Center for Nanoscience and Technology (NCNST), Beijing, P.R. China, 100190.

[∥]Institute of Chemistry, Chinese Academy of Sciences, Beijing, P. R. China, 100190.

Notes

The authors declare no competing financial interest.

[⊥]Also at Department of Chemistry, King Abdulaziz University, Jeddah 21589, Saudi Arabia.

■ ACKNOWLEDGMENTS

The work at Georgia Tech has been funded by the National Science Foundation under its STC Program (Award No. DMR-0120967) and (for part of the computational resources) under its CRIF Program (Award No. CHE-0946869). B.C. and T.R.C. acknowledge the National Science Foundation (Award No. CHE-0911690) for support. The authors warmly thank Prof. Mohammad Omary (UNT Chemistry) for inspiring this work and for stimulating discussions.

■ REFERENCES

(1) Dias, H. V. R.; Diyabalanage, H. V. K.; Rawashdeh-Omary, M. A.; Franzman, M. A.; Omary, M. A. Bright Phosphorescence of a Trinuclear Copper(I) Complex: Luminescence Thermochromism, Solvatochromism, and Concentration Luminochromism. *J. Am. Chem. Soc.* **2003**, *125*, 12072−12073.

(2) Dias, H. V. R.; Diyabalanage, H. V. K.; Eldabaja, M. G.; Elbjeirami, O.; Rawashdeh-Omary, M. A.; Omary, M. A. Brightly Phosphorescent Trinuclear Copper(I) Complexes of Pyrazolates: Substituent Effects on the Supramolecular Structure and Photophysics. *J. Am. Chem. Soc.* **2005**, *127*, 7489−7501.

(3) Omary, M. A.; Rawashdeh-Omary, M. A.; Gonser, M. W. A.; Elbjeirami, O.; Grimes, T.; Cundari, T. R.; Diyabalanage, H. V. K.; Gamage, C. S. P.; Dias, H. V. R. Metal Effect on the Supramolecular Structure, Photophysics, and Acid−Base Character of Trinuclear Pyrazolato Coinage Metal Complexes. *Inorg. Chem.* **2005**, *44*, 8200−8210.

(4) Caseri, W. R.; Chanzy, H. D.; Feldman, K.; Fontana, M.; Smith, P.; Tervoort, T. A.; Goossens, J. G. P.; Meijer, E. W.; Schenning, A. P. H. J.; Dolbnya, I. P.; et al. "(Hot-)Water-Proof", Semiconducting, Platinum-Based Chain Structures: Processing, Products, and Properties. *Adv. Mater.* **2003**, *15*, 125−129.

(5) Debije, M. G.; de Haas, M. P.; Warman, J. M.; Fontana, M.; Stutzmann, N.; Kristiansen, M.; Caseri, W. R.; Smith, P.; Hoffmann, S.; Sølling, T. I. Optoelectronic Properties of Quasi-Linear, Self-Assembled Platinum Complexes: Pt−Pt Distance Dependence. *Adv. Funct. Mater.* **2004**, *14*, 323−328.

(6) Vickery, J. C.; Olmstead, M. M.; Fung, E. Y.; Balch, A. L. Solvent-Stimulated Luminescence from the Supramolecular Aggregation of a Trinuclear Gold(I) Complex that Displays Extensive Intermolecular Au−Au Interactions. *Angew. Chem., Int. Ed.* **1997**, *36*, 1179−1181.

(7) White-Morris, R. L.; Olmstead, M. M.; Attar, S.; Balch, A. L. Intermolecular Interactions in Polymorphs of Trinuclear Gold(I) Complexes: Insight into the Solvoluminescence of $Au^I_3(MeN{=}COMe)_3$. *Inorg. Chem.* **2005**, *44*, 5021−5029.

(8) Winkler, K.; Wysocka-Zolopa, M.; Recko, K.; Dobrzynski, L.; Vickery, J. C.; Balch, A. L. Formation of a Partially Oxidized Gold Compound by Electrolytic Oxidation of the Solvoluminescent Gold(I) Trimer, $Au_3(MeN{=}COMe)_3$. *Inorg. Chem.* **2009**, *48*, 1551−1558.

(9) Mendizabal, F.; Aguilera, B.; Olea-Azar, C. Theoretical Study on Electronic Spectra and Aurophilic Attraction in $[Au_3(MeN{=}COMe)_3]_n$ (n = 1−4) Complexes. *Chem. Phys. Lett.* **2007**, *447*, 345−351.

(10) Mendizabal, F.; Burgos, D.; Olea-Azar, C. Theoretical Study of Electronic Spectra of $[Pt_3(\mu\text{-}CO)_3(CO)_3]_n^{-2}$ (n = 3−5) Complexes. *Int. J. Quantum Chem.* **2009**, *109*, 477−482.

(11) Blöchl, P. E. Projector Augmented-Wave Method. *Phys. Rev. B* **1994**, *50*, 17953−17979.

(12) Kresse, G.; Joubert, D. From Ultrasoft Pseudopotentials to the Projector Augmented-Wave Method. *Phys. Rev. B* **1999**, *59*, 1758−1775.

(13) Kresse, G.; Furthmüller, J. Efficiency of Ab-Initio Total Energy Calculations for Metals and Semiconductors Using a Plane-Wave Basis Set. *Comput. Mater. Sci.* **1996**, *6*, 15−50.

(14) Valeev, E. F.; Coropceanu, V.; da Silva Filho, D. A.; Salman, S.; Brédas, J.-L. Effect of Electronic Polarization on Charge-Transport Parameters in Molecular Organic Semiconductors. *J. Am. Chem. Soc.* **2006**, *128*, 9882−9886.

(15) Frisch, M. J.; Trucks, G. W.; Schlegel, H. B.; Scuseria, G. E.; Robb, M. A.; Cheeseman, J. R.; Montgomery, J. A. Jr.; Vreven, T.; Kudin, K. N.; Burant, J. C. et al. *Gaussian 09*, revision B. 01; Gaussian, Inc.: Wallingford CT, 2009.

(16) Coropceanu, V.; Li, Y.; Yi, Y.; Zhu, L.; Brédas, J.-L. Intrinsic Charge Transport in Single Crystals of Organic Molecular Semiconductors: A Theoretical Perspective. *MRS Bull.* **2013**, *38*, 57−71.